Transactions on Modelling and Simulation vol 3, © 1993 WIT Press, www.witpress.com, ISSN 1743-355X

Use of local reanalysis and quadratic h-hierarchical functions in adaptive boundary element models

A. Charafi, A.C. Neves, L.C. Wrobel
Wessex Institute of Technology, University of Portsmouth, Ashurst Lodge, Ashurst, Southampton, SO4 2AA, UK

ABSTRACT

An adaptive boundary element scheme is developed using the concept of local reanalysis and quadratic h-hierarchical functions for the construction of near optimal computational models. The use of local reanalysis in the error estimation guarantees the reliability of the modeling process while the use of h-hierarchical elements guarantees the efficiency of the adaptive algorithm. The technique is developed for the elastic analysis of two-dimensional models. A practical example of a microstructure component shows the rapid convergence of the results with few refinement steps.

INTRODUCTION

Adaptivity is the availability of a reliable error analysis allowing the discretized model to be selectively refined and thus improved. In more precise terms Rank [1] states that the key to adaptivity is " $\cdots$ a more or less accurate knowledge about the size and distribution of the error for a given FEM or BIEM approximation. Usually this knowledge has to be extracted a posteriori from the numerical solution in the form of error indicators for the local error and error estimator for the global error in some norm ".

The refinement will be necessary when the solution obtained from the analysis is not satisfactory. The accuracy of the solution may be verified by use of error estimators, but engineering considerations may also be used to test the reliability of the results. Once it has been judged necessary to refine, error indicators are used to show where the refinement should occur.

The adaptive algorithm should be both reliable (*i.e.* the desired error control should be guaranteed) and efficient (*i.e.* the computational work should be minimal).

In this paper, the concept of local reanalysis is adopted in the error estimation to guarantee the reliability of the quadratic h–hierarchical adaptive scheme. The emphasis is on two–dimensional elastic problems.

h-HIERARCHICAL (QUADRATIC) SHAPE FUNCTIONS

The main idea behind the use of h-hierarchical [2], instead of standard, shape functions is to improve the efficiency of the adaptive algorithm, since the computational work spent in the build up of the matrix for one iteration is saved to be used in the next iteration. The accuracy obtained using either of the two types of shape functions is the same as they just represent two different bases for the same functional space.

To define quadratic h-hierarchical shape functions [3] one starts with the polynomials

$$N_1(\xi) = 0.5\xi(\xi - 1),$$

$$N_2(\xi) = 0.5\xi(\xi + 1),$$

$$N_3(\xi) = 1 - \xi^2,$$

to represent the approximate solution $\hat{\varphi}$, on a certain geometric element Γ_e that has been mapped to the interval $[-1, 1]$ by

$$\hat{\varphi}(\xi) = \sum_{c=1}^{3} N_c(\xi)\hat{\varphi}_c \, .$$

Let Λ be the number of hierarchical levels (*i.e.* the number of iterations in the adaptive procedure) and $\mathcal{H}_\lambda$ the list of integers indicating those pairs of h-hierarchical functions that are used in the current mesh (for each level λ there are at most $2^{\lambda-1}$ pairs). The approximate solution is then given by

$$\hat{\varphi}(\xi) = \sum_{c=1}^{3} N_c(\xi)\hat{\varphi}_c + \sum_{\lambda=1}^{\Lambda} \sum_{k \in \mathcal{H}_\lambda} [N_{\lambda,2k-1}(\xi)\hat{\varphi}_{\lambda,2k-1} + N_{\lambda,2k}(\xi)\hat{\varphi}_{\lambda,2k}] \qquad (1)$$

where

$$N_{\lambda,n}(\xi) = \begin{cases} N_3(t_{\lambda,n}(\xi)) & \text{if } \xi \in [a_{\lambda,n}, b_{\lambda,n}] \\ 0 & \text{otherwise} \end{cases}$$

$$a_{\lambda,n} = -1 + (n-1)\frac{1}{2^{(\lambda-1)}} \, ,$$

$$b_{\lambda,n} = a_{\lambda,n} + \frac{1}{2^{(\lambda-1)}} \, ,$$

and $t_{\lambda,n}$ is a one-to-one mapping from $[a_{\lambda,n}, b_{\lambda,n}]$ to $[-1,1]$ defined by

$$t_{\lambda,n}(\xi) = 2^{\lambda}(\xi + 1) - 2n + 1$$

Figure 1 shows shape functions of the 1st hierarchical level and two out of four for the 2nd hierarchical level.

It is important to notice that $\hat{\varphi}_{\lambda,n}$ does not represent the approximate solution $\hat{\varphi}$ at the new collocation points $\xi_{\lambda,n}$, but rather auxiliary unknowns. To obtain the actual value of $\hat{\varphi}$, these unknowns have to be computed and substituted into equation (1) at $\xi = \xi_{\lambda,n}$.

Also, due to the presence of $\hat{\varphi}_{\lambda,n}$ which do not have any physical meaning, the Cauchy principal values (CPV) at $\xi_{\lambda,n}$ have to be calculated with a direct method rather than indirectly (like using rigid body motion).

In the adaptive process the geometric elements are never modified. Their number is usually quite low as they only have to represent the geometry and boundary conditions $\bar{\varphi}_c$. On refined elements, other degrees of freedom and internal modes (bumps) are added to the original interval $[-1,1]$.

BEM FORMULATION FOR 2D LINEAR ELASTOSTATICS

The starting point for the direct BEM formulation for 2D elastostatics without body forces is the Somigliana's identity for displacements [4]

$$c_{ij}(P)u_j(P) + \int_{\Gamma} T^*_{ij}(P,Q)u_j(Q)d\Gamma(Q) = \int_{\Gamma} U^*_{ij}(P,Q)t_j(Q)d\Gamma(Q) \qquad i,j = 1,2 \qquad (2)$$

where P is the source point and Q is the field point lying on the boundary Γ. U^*_{ij} and T^*_{ij} are the kernel functions and u_j and t_j are the displacement and traction components respectively. $c_{ij}(P)$ are the free terms which depend only upon the local geometry of Γ at P and orientation with respect to global axes.

For the numerical implementation of equation (2), the boundary Γ is divided into q continuous quadratic elements Γ_b and equation (2) becomes

$$c_{ij}(P)u_j(P) + \sum_{b=1}^{q} \int_{\Gamma_b} T^*_{ij}(P,Q(\xi))u_j(\xi)J_b(\xi)d\xi =$$

$$\sum_{b=1}^{q} \int_{\Gamma_b} U^*_{ij}(P,Q(\xi))t_j(\xi)J_b(\xi)d\xi \quad i,j = 1,2$$

where $J_b(\xi)$ is the Jacobian of the one-to-one mapping between the curvilinear abscissa along Γ_b and the intrinsic coordinate ξ.

After application of the boundary conditions the whole set of linear equations in the current iteration of an adaptive process can be expressed in matrix form as

$$A_{11}x_1 = b_1$$

In the next iteration when new degrees of freedom corresponding to the h-hierarchical shape functions are added, the system of equations will have the form

$$\begin{bmatrix} A_{11} & A_{12} \\ A_{21} & A_{22} \end{bmatrix} \begin{bmatrix} x_1 \\ x_2 \end{bmatrix} = \begin{bmatrix} b_1 \\ b_2 \end{bmatrix}$$

where the matrices A_{11} and b_1 remain unchanged.

Special care in the numerical integration

In the first iteration of the adaptive process, for the case when P lies within Γ_b, the values of the free term $c_{ij}(P)$ and the integral that contains T^*_{ij}, which is strongly singular and therefore exists only if defined in the Cauchy principal value (CPV) sense, are calculated indirectly by using rigid body motion.

For the next iterations the values of $c_{ij}(P)$ and the singular integrals have to be calculated directly. Since the added collocation point P is located inside the subelement, the value of $c_{ij}(P)$ at $\xi_{\lambda,n}$ is given by

$$c_{ij}(\xi_{\lambda,n}) = \begin{bmatrix} 1/2 & 0 \\ 0 & 1/2 \end{bmatrix} N_{\lambda,n}(\xi_{\lambda,n})$$

The strongly singular integral is given according to Guiggiani [5] by:

$$\int_{\Gamma_b} T^*_{ij}(P, Q(\xi)) N_{\lambda,n}(\xi) J_b(\xi) d\xi = \int_{-1}^{1} \frac{h_{ij}(\xi) - h_{ij}(\xi_{\lambda,n})}{\xi - \xi_{\lambda,n}} d\xi + h_{ij}(\xi_{\lambda,n}) ln| \frac{1 - \xi_{\lambda,n}}{1 + \xi_{\lambda,n}} |$$

where

$$h_{ij}(\xi_{\lambda,n}) = T^*_{ij}(P, Q(\xi)) N_{\lambda,n}(\xi) J_b(\xi)(\xi - \xi_{\lambda,n})$$

is a continuous regular function in $[-1, 1]$.

The quantity $h_{ij}(\xi_{\lambda,n})$ assumes the following values

$$h_{ij}(\xi_{\lambda,n}) = N_{\lambda,n}(\xi_{\lambda,n}) \begin{bmatrix} 0 & -\frac{1-2\nu}{4\pi(1-\nu)} \\ \frac{1-2\nu}{4\pi(1-\nu)} & 0 \end{bmatrix}$$

Thus, each CPV integral is reduced to a regular integral plus a simple closed-form-term. Notice that the use of Telles transformation [6] in the regular integral avoids ξ being coincident with $\xi_{\lambda,n}$.

In all preceding numerically calculated boundary integrals, Telles' transformation [6] is used. This transformation bunches the integration points closer to the singularity by using a third degree polynomial transformation allowing a smaller number of integration points for the same accuracy. Furthermore, Telles' transformation gives better results than if Gaussian quadrature is applied directly, and permits the computation of terms with singularities of order $O(\ln(r))$.

In the h–hierarchical adaptive process, special care should be taken when the source point is located close or inside a large element (usually the original element). As a general rule, increasing the number of integration points in the calculation of the boundary integrals provides improved accuracy of results. On the other hand, as this number increases, the computer program becomes less efficient. The method of selective integration [7] ensures an optimal balance between accuracy and efficiency using the minimum necessary number of integration points over the element situated at a certain distance from the source point.

The optimal number of integration points for a required accuracy depends on the relative position of the source point to the boundary element along which integration is carried out. The minimum distance required for a given number of integration points adopted in the program is given in Table 1.

	No. of integration points						
Location of P	4	6	8	10	16	32	64
Boundary Γ	4.0	1.4	0.7	0.4	0.18	0.05	0.

Table 1: Minimum distance D required against number of integration points.

THE PRINCIPLE OF LOCAL REANALYSIS

To assess the reliability of the modeling process an interpolation-type a posteriori error estimation is developed using the principle of local reanalysis. Before we define what is meant by " local reanalysis " it is worth investigating how one can estimate the error in a boundary integral equation. For that, let us consider a boundary integral equation of the form

$$\mathcal{K}\varphi \equiv \int_{\Gamma} K(s,t)\varphi(t)dt = f(s) \, .$$

The boundary Γ is subdivided into a certain number of elements and the exact solution approximated on each element Γ_e by

$$\varphi(s) \simeq \hat{\varphi}(s) = \sum_{k=1}^{n_e} N_k(s)\hat{\varphi}_k \, ,$$

where

n_e is the number of degrees of freedom on element Γ_e;

$\{N_k\}_{k\geq 1}$ are piecewise polynomials basis functions;

$\{\hat{\varphi}_k\}_{k\geq 1}$ are nodal values of the approximation $\hat{\varphi}$ to be determined.

The residual function is defined by

$$r(s) = \mathcal{K}\hat{\varphi} - f(s) \, , \text{ for } s \in \Gamma \, .$$

In the collocation method, the residual function is set to zero at all the n boundary nodes

$$r(s_i) = 0 \ , \ i = 1, 2, \ldots, n \ .$$

This leads to a system of equations to be solved. The nodal values $\{\hat{\varphi}_k\}_{k\geq 1}$ are then obtained and thus the approximation $\hat{\varphi}$ determined.

In this approach, starting from the assumption that a local change in the mesh will affect the solution only if the latter is not accurate enough, we introduce the concept of local reanalysis to measure the sensitivity of the solution once the mesh has been locally modified. In what follows we explain the concept of local reanalysis.

After the first approximation $\hat{\varphi}$ is obtained, we need to test its quality. The following discrete representation of the equation $\mathcal{K}\varphi = f$ is then obtained

$$\sum_{j=1}^{m} \int_{\Gamma_j} K(s_i, t)\hat{\varphi}(t)dt = f(s_i) \ , \text{ for } i = 1, \ldots, n \ ,$$

where m is the number of elements on the boundary Γ and n the number of collocation points.

Suppose that element Γ_j has been selected for reanalysis. The previous equation can then take the form:

$$a_i + \int_{\Gamma_j} K(s_i, t)\tilde{\varphi}(t)dt = f(s_i) \ ,$$

with s_i being any node on the element Γ_j, $\tilde{\varphi}$ the predicted solution on the element Γ_j calculated during local reanalysis; and a_i given by

$$a_i = \sum_{l \neq j} \int_{\Gamma_l} K(s_i, t)\hat{\varphi}(t)dt \ .$$

The values of φ on the portion $\Gamma - \Gamma_j$ of the boundary are supposed to be known from $\hat{\varphi}$, thus a_i is considered as known and the only unknowns $\tilde{\varphi}$ are on the element Γ_j. One discretizes only the element Γ_j into two subelements with n_{Γ_j} nodal points (if quadratic elements are used $n_{\Gamma_j} = 5$, see Figure 2), and solves the equation

$$\int_{\Gamma_j} K(s_i, t)\tilde{\varphi}(t)dt = g(s_i) = f(s_i) - a_i \ , \text{ for } i = 1, \ldots, n_{\Gamma_j} \ .$$

This produces a very small system relative to the one obtained when doing the analysis on all the boundary since the degrees of freedom are only those on the portion Γ_j of the boundary Γ. Hence, local reanalysis is relatively quick to perform. This idea has been first suggested by Casale [8] in his dissertation thesis. Its use as an error estimator has already proved reliable in the case of

potential problems [9]. Figure 3 shows how the local system of equations for the local reanalysis is obtained from the global one.

Local reanalysis is achieved over each element by refining the approximation over the element considered; computing a new solution by assuming that the boundary values on all the other elements are already known; and comparing it to the previous one providing a quick feedback on the quality of the solution. The use of local reanalysis enables us to build an error estimate – substituting the exact solution by the one obtained from the local reanalysis – which provides a measure of how the solution is affected by a local change in the mesh.

ERROR INDICATORS

After performing the local reanalysis over each element of the boundary we get a predicted solution $\tilde{\varphi}$. If $\hat{\varphi}$ is the numerical solution obtained from the standard boundary element analysis, the exact error is then approximated by $\Delta\varphi = \tilde{\varphi} - \hat{\varphi}$.

Error indicators are defined by measuring – in the L_2-norm – the difference between the two solutions $\hat{\varphi}$ and $\tilde{\varphi}$. The basic (although empirical) idea is that the difference between the two solutions is an indication of how sensitive is the solution $\hat{\varphi}$ to a local change in the mesh, providing some information about where the refinement should occur.

Assuming a uniform distribution of the error on the boundary Γ, the relative error percentage on the element Γ_i is defined by

$$\tau_{\varphi}^{i} = \left(\frac{n \ \|\Delta\varphi\|_i^2}{\|\hat{\varphi}\|^2 + \|\Delta\varphi\|^2} \right)^{\frac{1}{2}} \times 100\% \, ,$$

where n is the number of elements in the mesh.

The self–adaptive mesh refinement strategy is controlled by specifying for all elements

$$\tau_{\varphi}^{i} \leq \bar{\tau}_L \, ,$$

where $\bar{\tau}_L$ is a user–specified tolerance. It is important to notice that $\bar{\tau}_L$ is a local requirement.

For linear elasticity problems one needs to look at the convergence of the displacements and stresses. Convergence of the stresses implies that of displacements whereas the converse is not true.To provide a stable error indicator the error in Von Mises stresses

$$\sigma_{vm} = \sqrt{\sigma_{11}^2 + \sigma_{22}^2 + \sigma_{33}^2 + 3\sigma_{12}^2 - (\sigma_{11}\sigma_{22} + \sigma_{11}\sigma_{33} + \sigma_{22}\sigma_{33})}$$

has been used.

Two sets of values of the stress tensor have to be computed : $\hat{\sigma}$ obtained from the values of $\hat{u} = (\hat{u}_1, \hat{u}_2)$ and $\hat{t} = (\hat{t}_1, \hat{t}_2)$, and $\tilde{\sigma}$ obtained from the values of $\tilde{u} =$

$(\tilde{u}_1, \tilde{u}_2)$ and $\tilde{t} = (\tilde{t}_1, \tilde{t}_2)$. To compute the stress tensor values on the boundary the approach described by Lachat [10] is used. First, the local stresses are calculated using a finite difference scheme and then, a transformation is carried out to obtain the global values of the stress tensor from the local ones. The error indicators for the Von Mises stress are defined as

$$\tau^i(\sigma_{vm}) = \left(\frac{n \, ||\Delta\sigma_{vm}||_i^2}{||\hat{\sigma}_{vm}||^2 + ||\Delta\sigma_{vm}||^2} \right)^{\frac{1}{2}} \times 100\% \, .$$

STOPPING CRITERIA

The refinement procedure can be terminated by use of different stopping criteria:

- If $\tau_\varphi^i \leq \bar{\tau}_L$ for all elements.
- By specifying an error bound $\bar{\tau}_G$ for the global error percentage of the solution, if one is interested in the global accuracy:

$$\tau_{\varphi_1} = \left(\frac{||\Delta\varphi||^2}{||\hat{\varphi}||^2 + ||\Delta\varphi||^2} \right)^{\frac{1}{2}} \times 100\% \leq \bar{\tau}_G \, ,$$

  However, one should keep in mind that a good overall accuracy could well mask large errors in small parts of the boundary.

- By storage considerations, that is, by specifying the maximum number of degrees of freedom the user is prepared to include in the analysis.
- By time limitation considerations specifying, for example, a maximum number of re–solutions.
- By studying the constants of a boundary value problem like the global equilibrium or the norm $||\varphi||$, namely

$$\tau_{\varphi_2} = \frac{| \, ||\hat{\varphi}^{k+1}|| - ||\hat{\varphi}^k|| \, |}{||\hat{\varphi}^k||} \times 100\% \leq \bar{\tau}_G .$$

  where k and $k+1$ represent two successive iterations.

ADAPTIVE STRATEGY

The adaptive refinement strategy is described by the following algorithm:

Step 1–Define shape and boundary conditions

Step 2–Perform standard BEM analysis using h-hierarchical functions

Step 3–Compute the norm of the solution $||\hat{\varphi}||$

Step 4–Local reanalysis:

* Subdivide the element
* Form the small system of equations $AX = B$
* Solve the system of equations
* Compute the norms of the local errors $||\Delta\varphi|| = ||\tilde{\varphi} - \hat{\varphi}||$

Step 5–Compute the global percentage errors:

$$\tau_{\varphi_1} = \left(\frac{||\Delta\varphi||^2}{||\hat{\varphi}||^2 + ||\Delta\varphi||^2} \right)^{\frac{1}{2}} \times 100\% ,$$

$$\tau_{\varphi_2} = \frac{| \, ||\hat{\varphi}^{k+1}|| - ||\hat{\varphi}^k|| \, |}{||\hat{\varphi}^k||} \times 100\% ,$$

Step 6–Compute the local percentage errors on the elements Γ_i:

$$\tau_{\varphi}^{i} = \left(\frac{n \, ||\Delta\varphi||_i^2}{||\hat{\varphi}||^2 + ||\Delta\varphi||^2} \right)^{\frac{1}{2}} \times 100\%,$$

Step 7–If one of the stopping criteria is satisfied, then STOP,

else subdivide the elements Γ_i for which: $\tau_{\varphi}^{i} > \bar{\tau}$, and Go to step 2

NUMERICAL APPLICATION

The proposed adaptive scheme has been applied to a practical $2D$ study of an accelerometer hinge submitted to a prescribed displacement. This device measures the acceleration of bodies, utilizing capacity effects caused by its deformation in an electrical field. The geometry, boundary conditions and corresponding deformed shape are shown in Figure 4. The hinge is fixed at the lower block by prescribing zero displacement in both directions at point B and in the x_2 direction at point C. The upper block is bent in the x_1 direction by applying a displacement of magnitude $-0.01mm$ at point A. The material properties are $E = 1.9 \times 10^5 N/mm^2$ and $\nu = 0.31$.

Considering a local tolerance $\bar{\tau}_L = 0.5\%$ and a global tolerance $\bar{\tau}_G = 0.05\%$, the meshes in the adaptive process are shown in Figure 5. As expected, a high graded refinement occurs in the thinner area of the structure.

The maximum Von Mises stress obtained by the present adaptive analysis is compared with BEASY (554 boundary elements) and ANSYS results (a very fine finite element mesh) in Table 2. In all the analyses, the maximum stress occurs in the same region. Figure 6 shows the contour plot obtained by BEASY analysis.

	Present Adaptive Scheme				BEASY	ANSYS
No. of elements	66	82	106	138	554	—
Max. σ_{vm}	26.628	27.316	28.631	28.838	28.941	28.940

Table 2 : Maximum Von Mises stress.

The values of the global error estimator τ_{φ_1} and the stopping criteria τ_{φ_2} (for $\varphi = \sigma_{vm}$) are shown in Table 3.

Mesh	No. Elements	τ_{φ_1}	τ_{φ_2}
1	66	4.788 %	—
2	82	1.576 %	0.829 %
3	106	0.553 %	0.509 %
4	138	0.219 %	0.111 %

Table 3: Parameters of the adaptive procedure.

CONCLUSION

A new quadratic h-hierarchical adaptive strategy for boundary element method using error estimation based on the concept of local reanalysis has been proposed for the construction of near-optimal computational models. The use of local reanalysis in the posteriori error estimation guarantees the reliability of the modeling process while the use of h-hierarchical shape functions over the elements guarantees the efficiency of the adaptive algorithm, since the computational work spent in the build up of the matrix for one iteration is saved to be used in the next iteration.

In order to avoid excessive integration errors when the length of the sub-element is very small compared to the original one, and to increase the efficiency of the numerical integration, Telles' transformation is used in conjunction with a selective integration scheme.

The proposed adaptive strategy has proved to be successful in solving practical problems and produced good results with much fewer elements than standard non-adaptive boundary element or finite element codes.

It is the authors' belief that successful solutions of the two basic problems in adaptivity (reliability and efficiency) will have a profound influence on the boundary element software of tomorrow.

ACKNOWLEDGMENT

This research forms part of the European Commission ESPRIT project 6874, Microsystem Analysis and Simulation System (MASS), with partners Wessex Institute of Technology, Technical University Berlin, Computational Mechanics BEASY and MicroParts. The accelerometer hinge analysed here was designed by MicroParts. Results from BEASY and ANSYS were obtained by Dr. A. Larhmann from TUB. BEASY is a product of Computational Mechanics BEASY. ANSYS is a product of Swanson Analysis Ltd.

References

[1] Rank E., *Adaptive h–, p–, and hp–versions for boundary element methods*, Int. J. Num. Meth. Eng., Vol. 28, pp. 1335–1349, (1989).

[2] Parreira P., *Análise do erro no método dos elementos de fronteira em elasticidade*, PhD thesis, Instituto Superior Técnico, Lisbon, (1987).

[3] Guiggiani M., Lombardi, F. *Self-adaptive boundary elements with* h-*hierarchical shape functions*, Advances in Eng. Software, Vol. 15, pp 269-277, (1992).

[4] Somigliana, C., *Sopra l'Equilibrio di un Corpo Elastico Isotropo*, Il Nuovo Ciemento, pp 17-19, (1885).

[5] Guiggiani M., *Error indicators for adaptive mesh refinement in the boundary element method. A new approach*, Int. J. Num. Meth. Eng., Vol. 29, pp. 1247–1269, (1990).

[6] Telles J. C. F., *A self-adaptive coordinate transformation for efficient numerical evaluation of general boundary element integrals*, Int. J. Num. Meth. Eng., Vol. 24, pp. 959–973, (1987).

[7] Neves, A.C. and Brebbia, C.A., *Selective integration for 2-D elastic problems* Eng. Anal. with Boundary Elements, Vol. 9, pp 99-104, (1992).

[8] Casale M., *The integration of geometric modeling and structural analysis using trimmed patches*, PhD thesis, University of California, Irvine, (1989).

[9] Charafi A., Wrobel L. C. and Adey R., *An approach to h–adaptive boundary element methods using local reanalysis*, in 7th Int. Conf. on Boundary Element Technology, University of New Mexico in Albuquerque, U. S. A., Computational Mechanics Publications, (1992).

[10] Lachat J. C., *A further development of the boundary integral technique for elastostatics*, PhD thesis, University of Southampton, U. K., (1975).

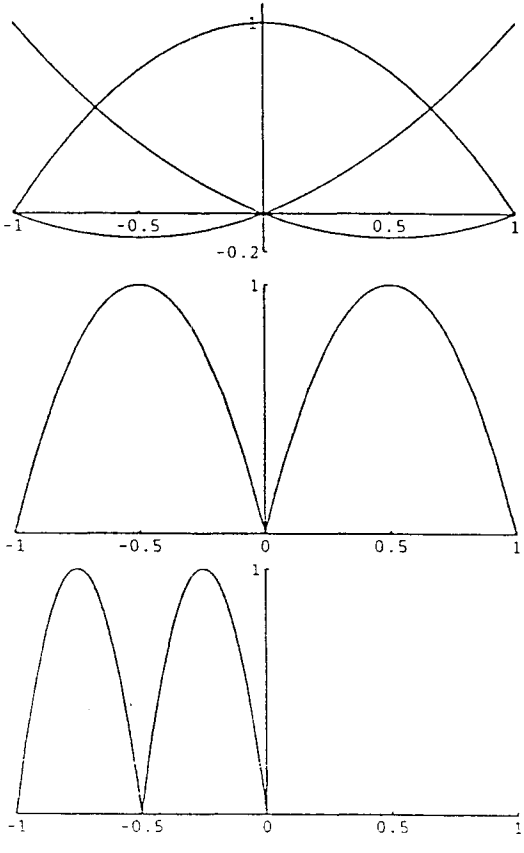

Figure 1: Quadratic h-hierarchical shape functions: $\lambda = 1$ and $\mathcal{H}_\lambda = 1$; $\lambda = 2$ and $\mathcal{H}_\lambda = 1$.

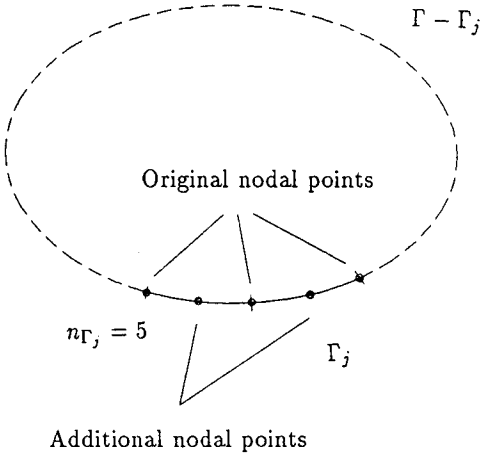

Figure 2: Local discretization for local reanalysis.

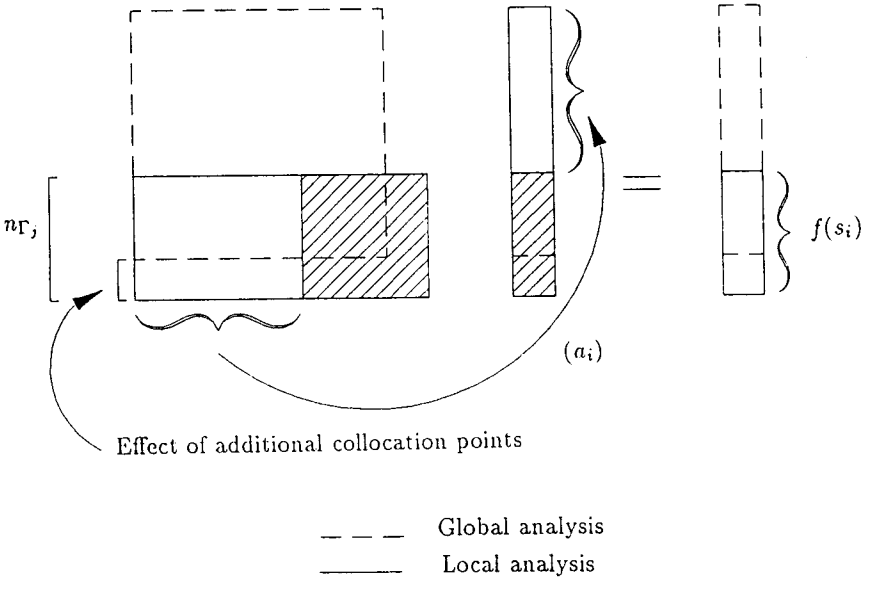

Figure 3: Matrix illustration of local reanalysis.

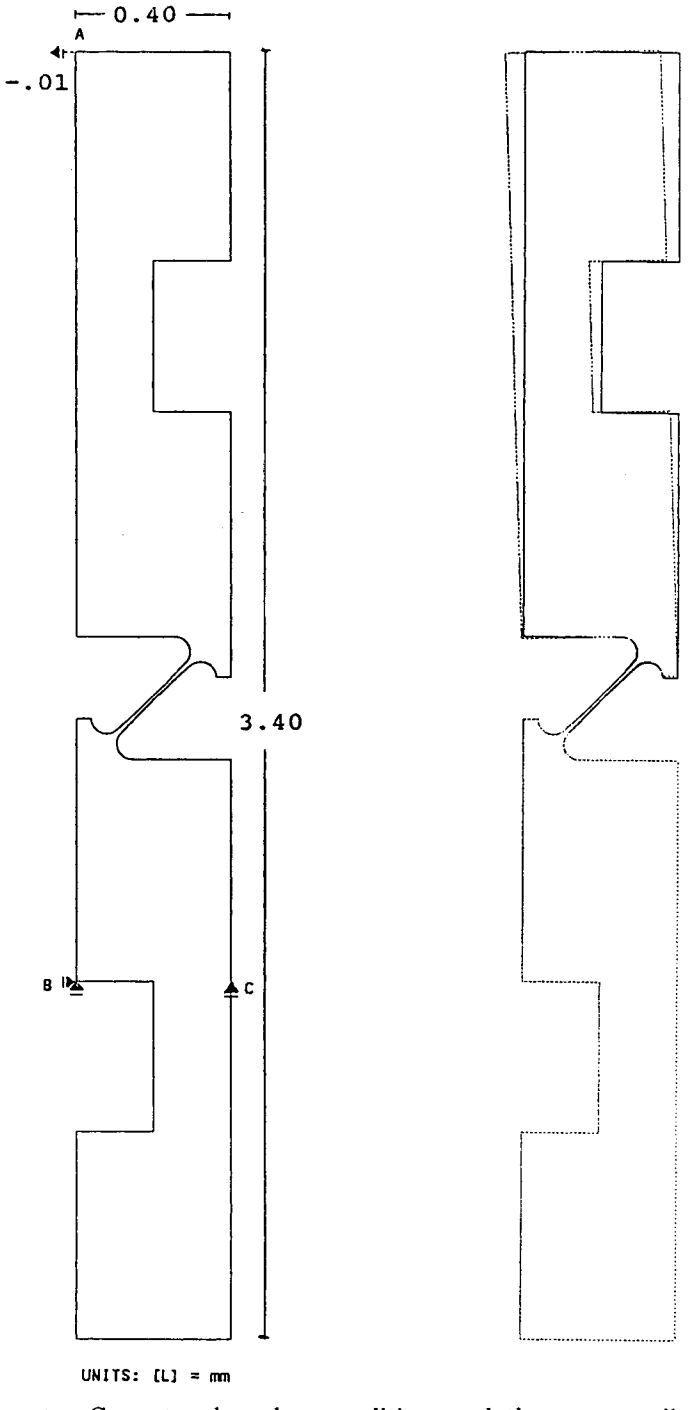

Figure 4: Geometry, boundary conditions and the corresponding deformed shape of the accelerometer hinge.

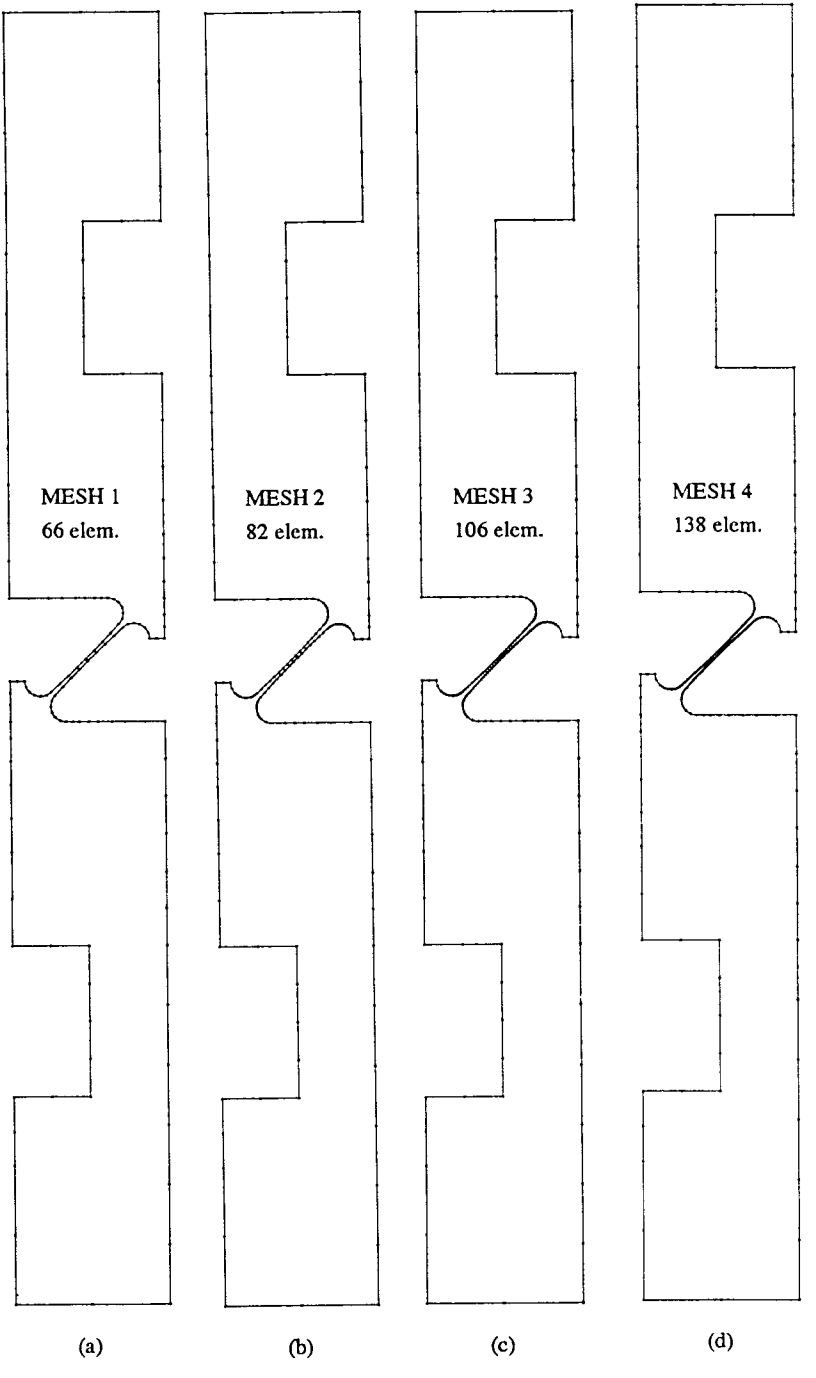

Figure 5: Adaptive meshes of the accelerometer hinge.

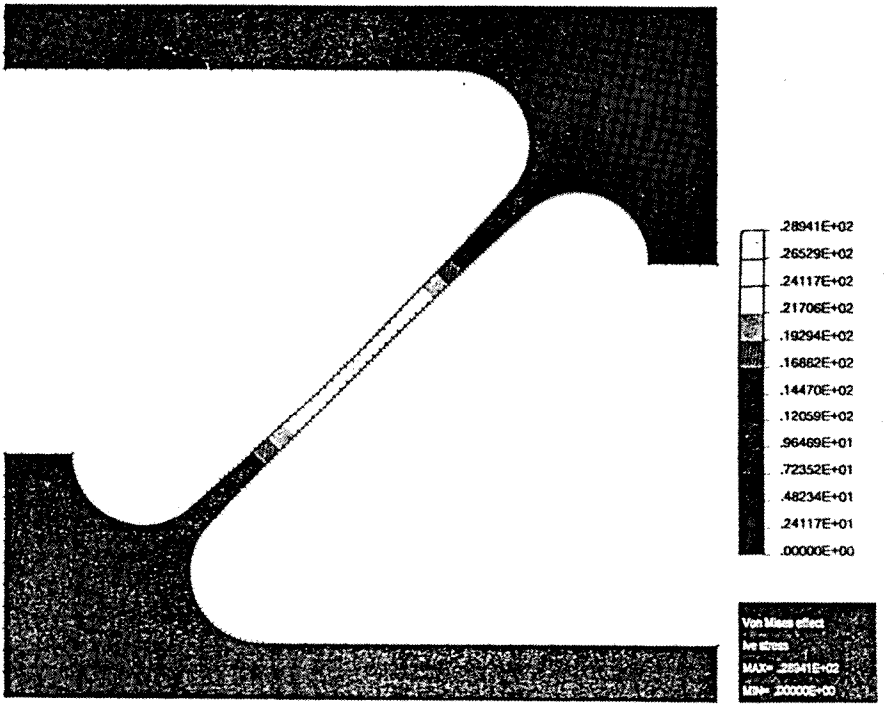

Figure 6: Contour plot of the Von Mises stresses using BEASY analysis.